Ruth V. Sabariego graduated in telecommunication engineering in 1998 at the University of Vigo, Spain. She received the PhD degree in applied sciences from the University of Lige, Belgium, in 2004. From 1998 till 2000, she was a research assistant at the Dept. of Communication Technology, University of Vigo, Spain. In October 2000, she joined the Unit of Applied Electricity (ELAP), Dept. of Electrical Engineering and Computer Science, University of Lige, Belgium. Here, she keeps on devoting her research to the domain of applied mathematics in computational electromagnetics. Particular applications are the modelling of eddy current non-destructive testing and microelectromechanical devices (MEMS).

Patrick Dular received the electrical engineer degree and Ph.D. degree in applied science from the University of Lige, Belgium, in 1990 and 1994, respectively. Here is currently with the Department of Electrical Engineering and Computer Science, University of Lige, as a Research Associate with the Belgian National Fund for Scientific Research (F.N.R.S.). His research mainly deals with the numerical modeling of coupled problems in electromagnetic systems, including both physical models and numerical techniques coupling.

$h-$ and $b-$conform finite element perturbation techniques for nondestructive eddy current testing

Ruth V. Sabariego and Patrick Dular

University of Liége, Dept. of Electrical Engineering and Computer Science (ELAP), B-4000 Liége, Belgium
E-mail: R.Sabariego@ulg.ac.be

Abstract

Purpose – The aim of the present paper is to compare the performances of a finite-element perturbation technique applied either to the $\boldsymbol{h}-$conform magnetodynamic formulation or to its $\boldsymbol{b}-$conform counterpart in the frame of nondestructive eddy-current testing (ECT) problems.

Design/methodology/approach/ – In both complementary perturbation techniques, the computation is split into a computation without defect (unperturbed problem) and a computation of the field distorsion due to its presence (perturbation problem). The unperturbed problem is conventionally solved in the complete domain. The source of the perturbation problem is then determined by the projection of the unperturbed solution in a relatively small region surrounding the defect. The discretisation of this reduced domain is chosen independently of the dimensions of the excitation probe and the specimen under study and is thus well adapted to the size of the defect.

Findings – The accuracy of the perturbation model is evidenced by comparing the results of the two counterpart formulations for different dimensions of the reduced domain to those achieved in the conventional way. The size of the reduced domain increases with the size of the defect at hand. This proposed sub-domain approach eases considerably the meshing process and speeds-up the computation for different probes positions.

Originality/Value – At a discrete level, the impedance change due to the defect is efficiently and accurately computed by integrating only over the defect itself and a layer of elements in the reduced domain that touches its boundary. Therefore, no integration of any flux variation in the coils is required.

Keywords Perturbation technique, finite element method, nondestructive testing, eddy currents

Paper type Research paper

Introduction

The ultimate goal of nondestructive eddy-current testing (ECT) problems is to determine the position and size of defects in conducting materials (inverse problem). However, a fast and accurate calculation of the probe response (forward problem) is often required for identifying the flaws from measured data. When the excitation is time-harmonic, the observed quantity is usually the impedance variation due to the presence of the defect.

Several variations of the volume integral method (VIM) have been reported in literature (**?**; **?**) for solving this kind of problems. Herein, defects are represented by a distribution of current dipoles in its volume. A boundary element method with a VIM characterisation of the defect is proposed in (**?**). Given that only the crack is discretised, the calculations associated to the different probe positions are very fast. Nevertheless, these techniques become extremely expensive in case of complicated geometries other than infinite stabs or tubes with homogeneous and linear material parameters.

The finite element method (**?**) allows to overcome these drawbacks. However, it may require a dense discretisation in the vicinity of the defect resulting in a large 3D mesh. The impedance variation due to the defect is calculated as the difference of the impedance values with and without flaw. Further, calculations for different probe positions are performed independently, which is time consuming.

An $\boldsymbol{h}-$conform finite element scheme that calculates directly the eddy-current distortion due to a flaw was proposed by the authors in (**?**). Herein, the computation is split into a computation without flaw and a computation of the field distortion due to its presence. The unperturbed field is calculated in a large region taking advantage of any symmetry or analytical solution, and applied as a source in the flaw for the second computation. The perturbed field can thus be determined in a reduced domain around the defect, what allows for a discretisation better adapted to its size.

This paper compares the $\boldsymbol{h}-$conform perturbation technique with its $\boldsymbol{b}-$conform counterpart. An expression for the impedance variation is derived for both considered formulations. As test case, the second benchmark problem proposed by the WFNDEC (**?**) is considered. It concerns a tube with a crack on its outer surface which is scanned by a probe placed inside it.

Perturbation method

We consider a magnetodynamic problem in a bounded domain Ω (boundary Γ) of $\mathbb{R}^3$. The eddy current conducting part of Ω is denoted Ω_c and the non-conducting one Ω_c^C ($\Omega = \Omega_c \cup \Omega_c^C$). Source conductors, with a given current density $\boldsymbol{j}_s$, are comprised in $\Omega_s \subset \Omega_c^C$. A flaw Ω_f (boundary Γ_f) appears in Ω_c. The source term of the perturbation formulation is obtained from the eddy-current distribution without defect.

For the sake of simplicity, let us assume hereafter a zero-conductivity flaw $\sigma_f = 0$ with the same magnetic permeability $\mu_f = \mu$ as the host material. Further both are linear and isotropic. Particularising the Ampère law for the unflawed (subscript

This work is supported by the Belgian Science Policy (IAP P6/21) and the Belgian French Community (ARC 03/08-298). P. Dular is a Research Associate with the Belgian National Fund for Scientific Research (F.N.R.S.).

u) and flawed (subscript f) arrangements, $\operatorname{curl} \boldsymbol{h}_u = \sigma \boldsymbol{e}_u$ and $\operatorname{curl} \boldsymbol{h}_f = 0$, respectively, where $\boldsymbol{h}$ and $\boldsymbol{e}$ are the magnetic and electric fields. Subtracting these two expressions, we obtain

$$\operatorname{curl} \boldsymbol{h} = \boldsymbol{j}_{sf} = -\sigma \boldsymbol{e}_u = -\operatorname{curl} \boldsymbol{h}_u \,, \tag{1}$$

with $\boldsymbol{h} = \boldsymbol{h}_f - \boldsymbol{h}_u$ the perturbation magnetic field and $\boldsymbol{j}_{sf}$ the source electric current density generating the perturbation (**?**).

h–*magnetodynamic formulation*

The $\boldsymbol{h} - \phi$ magnetodynamic formulation is obtained from the weak form of the Faraday law:

$$\partial_t(\mu \boldsymbol{h}, \boldsymbol{h}')_\Omega + (\sigma^{-1} \operatorname{curl} \boldsymbol{h}, \operatorname{curl} \boldsymbol{h}')_{\Omega_c} + \langle \boldsymbol{n} \times \boldsymbol{e}, \boldsymbol{h}' \rangle_\Gamma = 0 \,, \quad \forall \boldsymbol{h}' \in F_{h\phi}(\Omega) \tag{2}$$

where $\boldsymbol{n}$ is the outward unit normal vector on Γ, part of the boundary of Ω; $(\cdot,\cdot)_\Omega$ and $\langle \cdot,\cdot \rangle_\Gamma$ denote a volume integral in Ω and a surface integral on Γ of the product of their arguments; $F_{h\phi}(\Omega)$ is the function space defined on Ω and containing the basis functions for $\boldsymbol{h}$ (coupled to ϕ) as well as for the test function $\boldsymbol{h}'$ (**?**). At the discrete level, this space is built with edge finite elements. The trace of $\boldsymbol{e}$ is a constraint associated with Γ (this constraint can e.g. be associated with a homogeneous natural boundary condition or with a global quantity) (**?**).

The unperturbed field $\boldsymbol{h}_u$ (with $\Omega_f \subset \Omega_c$) is obtained by particularising ($\boldsymbol{h} = \boldsymbol{h}_u$) and solving (**??**). This field $\boldsymbol{h}_u$ is then projected to a reduced domain $\Omega' \subset \Omega$ around the defect. Note that projecting only $\boldsymbol{h}_u$ is not enough. This way the local current $\boldsymbol{j}_u = \operatorname{curl} \boldsymbol{h}_u$ will not be conserved. Furthermore, the trace of source field $\boldsymbol{h}_{sf} = -\boldsymbol{h}_u$, $\boldsymbol{n} \times \boldsymbol{h}_{sf}$, on Γ_f contributes to the exterior domain $\Omega' \backslash \Omega_f$. Indeed, the following interface condition has to be satisfied on Γ_f

$$\boldsymbol{n} \cdot \boldsymbol{j} \,|_{\Gamma_f} = -\boldsymbol{n} \cdot \boldsymbol{j}_{sf} \,|_{\Gamma_f} \,, \tag{3}$$

which is equivalent to consider

$$\boldsymbol{n} \times \boldsymbol{h} \,|_{\Gamma_f} = -\boldsymbol{n} \times \operatorname{grad} \phi \,|_{\Gamma_f} + \boldsymbol{n} \times \boldsymbol{h}_{sf} \,|_{\Gamma_f} \ . \tag{4}$$

The source of the perturbation problem in Ω_f is calculated through a projection method in Ω' as

$$(\operatorname{curl} \boldsymbol{h}_{sf}, \operatorname{curl} \boldsymbol{h}')_{\Omega'} - (\boldsymbol{j}_{sf}, \operatorname{curl} \boldsymbol{h}')_{\Omega'} = 0 \,, \quad \forall \boldsymbol{h}' \in F_{h\phi}(\Omega'), \tag{5}$$

where a gauge condition using a tree-cotree method at the discrete level in Ω' is applied to ensure the uniqueness of the solution. Hereafter we refer to Ω' as Ω.

The perturbation problem is completely characterised by (**??**) applied to the perturbation field $\boldsymbol{h}$ and taking into account (**??**) as follows:

$$\partial_t(\mu \boldsymbol{h}, \boldsymbol{h}')_\Omega + (\sigma^{-1} \operatorname{curl} \boldsymbol{h}, \operatorname{curl} \boldsymbol{h}')_{\Omega_c \backslash \Omega_f} + \partial_t(\mu \boldsymbol{h}_{sf}, \boldsymbol{h}')_\Omega + (\boldsymbol{j}_{sf}, \operatorname{curl} \boldsymbol{h}')_{\Omega_f} = 0 \,, \quad \forall \boldsymbol{h}' \in F_{h\phi}(\Omega) \,. \tag{6}$$

Calculation of the impedance variation The final goal is to calculate the impedance variation of the probe which allows to detect and characterise the defect. However, the change of the observed quantity is usually under 1% of the total value or even smaller in practical cases. The accurate calculation of this impedance variation ΔZ is crucial.

Taking into account the developments presented in (**?**), ΔZ can be accurately obtained by performing an integral over the defect Ω_f and a layer of elements in $\Omega \backslash \Omega_f$ that touch Γ_f.

A suitable treatment of the surface integral term in (**??**) consists in naturally defining a global voltage U in a weak sense. We can define a global test function for $\boldsymbol{h}$ with a unit circulation along any current tube of the inductor so that the surface integral in (**??**) can be expressed as the product of a global voltage U and a unit global current $I(\operatorname{curl} \boldsymbol{h}')$(**?**).

Let us specify (**??**) for the unflawed problem, it holds

$$\partial_t(\mu \boldsymbol{h}_u, \boldsymbol{h}')_\Omega + (\sigma^{-1} \operatorname{curl} \boldsymbol{h}_u, \operatorname{curl} \boldsymbol{h}')_{\Omega_c} = U_u \, I(\operatorname{curl} \boldsymbol{h}'), \quad \forall \boldsymbol{h}' \in F_{h\phi}(\Omega). \tag{7}$$

Analogously, for the flawed problem, we can write

$$\partial_t(\mu \boldsymbol{h}_f, \boldsymbol{h}')_\Omega + (\sigma^{-1} \operatorname{curl} \boldsymbol{h}_f, \operatorname{curl} \boldsymbol{h}')_{\Omega_c \backslash \Omega_f} + (\boldsymbol{e}_f, \operatorname{curl} \boldsymbol{h}')_{\Omega_f} = U_f \, I(\operatorname{curl} \boldsymbol{h}'), \quad \forall \boldsymbol{h}' \in F_{h\phi}(\Omega), \tag{8}$$

where we have added the term $(\boldsymbol{e}_f, \operatorname{curl} \boldsymbol{h}')_{\Omega_f}$ which is not cancelled as in the general case due to the imposed perturbation current in the flaw, i.e. $\operatorname{curl} \boldsymbol{h}' \neq 0$ in $\Omega_f \subset \Omega_c^C$.

Choosing as test functions $\boldsymbol{h}' = \boldsymbol{h}_f$ in (**??**) and $\boldsymbol{h}' = \boldsymbol{h}_u$ in (**??**) and subtracting (**??**) from (**??**), we obtain

$$\Delta U \, I = \Delta Z \, I^2 == -(\sigma^{-1} \operatorname{curl} \boldsymbol{h}_u, \operatorname{curl} \boldsymbol{h}_f)_{\Omega_f} + (\boldsymbol{e}_f, \operatorname{curl} \boldsymbol{h}_u)_{\Omega_f} = (\boldsymbol{e}_f, \operatorname{curl} \boldsymbol{h}_u)_{\Omega_f} \,, \tag{9}$$

where the first volume integral cancels because $\boldsymbol{h}_f$ is curl-free in Ω_f and I is the real current injected in the inductor.

The perturbed electric field $\boldsymbol{e}_f$ is not known in the flaw but can be calculated by means of (**??**) with $\boldsymbol{h}' = \boldsymbol{h}_{sf}$. This way $I(\operatorname{curl} \boldsymbol{h}') = 0$ and the impedance variation ΔZ is obtained as

$$\Delta Z \, I^2 = (\boldsymbol{e}_f, \operatorname{curl} \boldsymbol{h}_u)_{\Omega_f} = -(\boldsymbol{e}_f, \operatorname{curl} \boldsymbol{h}_{sf})_{\Omega_f} = (\sigma^{-1} \operatorname{curl} (\boldsymbol{h} + \boldsymbol{h}_{sf}), \boldsymbol{j}_{sf})_{\Omega_c \backslash \Omega_f} + \partial_t(\mu(\boldsymbol{h} + \boldsymbol{h}_{sf}), \boldsymbol{h}_{sf})_\Omega \,, \tag{10}$$

where the domain of integration, at the discrete level, is actually limited to Ω_f and a layer of elements in $\Omega \backslash \Omega_f$ touching Γ_f due to the definition of $\boldsymbol{h}_{sf}$.

Consequently, no integration of any flux variation in the coils is required, which would not be directly accessible because of the lack of explicit solution there (no mesh of the coils for the perturbed problem).

a–*magnetodynamic formulation*

The $\boldsymbol{a}-$magnetodynamic formulation is obtained from the weak form of the Ampere law:

$$(\nu\,\mathrm{curl}\,\boldsymbol{a},\mathrm{curl}\,\boldsymbol{a}')_{\Omega}+(\sigma\,\partial_t\boldsymbol{a},\boldsymbol{a}')_{\Omega_c}+\langle\boldsymbol{n}\times\boldsymbol{h},\boldsymbol{a}'\rangle_{\Gamma}=0\,,\quad\forall\,\boldsymbol{a}'\in F_a(\Omega)\,,\tag{11}$$

where $\boldsymbol{a}$ is the magnetic vector potential; ν the reluctivity; $F_a(\Omega)$ is the function space defined on Ω and containing the basis functions for $\boldsymbol{a}$ as well as for the test function $\boldsymbol{a}'$ (**?**). At the discrete level, this space is built with edge finite elements. The trace of $\boldsymbol{h}$ is a constraint associated with Γ which can e.g. be associated with a homogeneous natural boundary condition or with a global quantity (**?**).

Analogously to the $\boldsymbol{h}-$conform formulation, the unperturbed magnetic vector potential $\boldsymbol{a}_u$ is obtained by particularising ($\boldsymbol{a}=\boldsymbol{a}_u$) and solving (**??**). This potential $\boldsymbol{a}_u$ is then projected to a reduced domain $\Omega'\subset\Omega$ around the defect. The interface condition (**??**) has to be satisfied on Γ_f. The source of the perturbation problem in Ω_f is directly calculated from the projected $\boldsymbol{a}_u$ as

$$\boldsymbol{j}_{sf}=\sigma\,\partial_t\boldsymbol{a}_u\,.\tag{12}$$

The perturbation problem is completely characterised by (**??**) applied to the perturbation magnetic vector potential $\boldsymbol{a}$ and taking into account (**??**) as follows:

$$(\nu\,\mathrm{curl}\,\boldsymbol{a},\mathrm{curl}\,\boldsymbol{a}')_{\Omega}+(\sigma\,\partial_t\boldsymbol{a},\boldsymbol{a}')_{\Omega_c\setminus\Omega_f}+(\sigma\boldsymbol{j}_{sf},\boldsymbol{a}')_{\Omega_f}=0\,,\quad\forall\,\boldsymbol{a}'\in F_a(\Omega)\,.\tag{13}$$

Calculation of the impedance variation Analogously to the $\boldsymbol{h}$-conform case, for the $\boldsymbol{b}-$conform formulation, a suitable treatment of the surface integral term in (**??**) consists in naturally defining a global current I in a weak sense. We can define a global test function for $\boldsymbol{a}$ with a unit flux through any cut of the inductor so that the surface integral in (**??**) can be expressed as the product of a global current I and a unit global voltage $U(a')$(**?**).

Let us specify (**??**) for the unflawed problem, it holds

$$(\nu\,\mathrm{curl}\,\boldsymbol{a}_u,\mathrm{curl}\,\boldsymbol{a}')_{\Omega}+(\sigma\,\partial_t\boldsymbol{a}_u,\boldsymbol{a}')_{\Omega_c}=I_u\,U(\boldsymbol{a}'),\quad\forall\,\boldsymbol{a}'\in F_a(\Omega).\tag{14}$$

Analogously, for the flawed problem, we can write

$$(\nu\,\mathrm{curl}\,\boldsymbol{a}_f,\mathrm{curl}\,\boldsymbol{a}')_{\Omega}+(\sigma\,\partial_t\boldsymbol{a}_f,\boldsymbol{a}')_{\Omega_c\setminus\Omega_f}+(\sigma\boldsymbol{e}_f,\boldsymbol{a}')_{\Omega_f}=I_f\,U(\boldsymbol{a}'),\quad\forall\,\boldsymbol{a}'\in F_a(\Omega).\tag{15}$$

where we have added the term $(\sigma\boldsymbol{e}_f,\boldsymbol{a}')_{\Omega_f}$ which is not cancelled as in the general case due to the imposed perturbation current in the flaw, i.e. $\sigma\neq 0$ in $\Omega_f\subset\Omega_c^C$.

Choosing as test functions $\boldsymbol{a}'=\boldsymbol{a}_f$ in (**??**) and $\boldsymbol{a}'=\boldsymbol{a}_u$ in (**??**) and subtracting (**??**) from (**??**), we can prove that

$$\Delta Z\,I^2=-(\boldsymbol{e}_f,\boldsymbol{j}_{sf})_{\Omega_f}=(\boldsymbol{e}_f,\sigma\partial_t\boldsymbol{a}_u)_{\Omega_f}=(\sigma\partial_t(\boldsymbol{a}+\boldsymbol{a}_u),\partial_t\boldsymbol{a}_u)_{\Omega_f}+(\nu\,\mathrm{curl}\,(\boldsymbol{a}+\boldsymbol{a}_u),\mathrm{curl}\,\boldsymbol{a}_u)_{\Omega}\,,\tag{16}$$

where the perturbed electric field $\boldsymbol{e}_f$ in Ω_f, analogously to the $\boldsymbol{h}-$formulation case, is calcultated through (**??**).

Application example

As numerical example, we consider the second eddy current benchmark problem proposed by the WFNDEC (**?**). It concerns an Inconel tube ($\sigma=10^6$ S/m, inner radius $R_i=9.845$ mm, outer radius $R_o=11.115$ mm) with a defect on the outer surface and a pancake coil that scans the inner surface (Figure **??**). The flaw is $t=1$ mm long in the axial direction, $w=3$ mm wide in the radial direction and its depth h varies between 20% and 60% of the tube wall thickness. The coil (400 turns, inner diameter = 1 mm, outer diameter = 3 mm, height = 0.8 mm) carries an imposed sinusoidal current of 100 mA and frequency $f=150$ kHz. The lift-off between the coil and the tube is 0.8 mm.

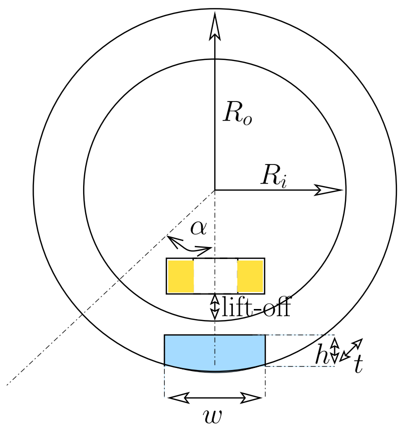

Figure 1. Cross section of the Incodel tube with a defect on the outer surface and a coil inside.

We define the size of the reduced domain Ω' in terms of the distance D (multiple of the skin depth $\delta = 1/\sqrt{\pi f \mu \sigma} = 1.3$ mm of the tube) from the boundary of the crack to the boundary of Ω'. We study the accuracy of the perturbation FE based method as a function of the size of Ω'. To this purpose, we vary the dimensions of Ω' as a function of the distance D. We calculate the impedance variation ΔZ both in the conventional way (solving the unflawed and the flawed problem consecutively and performing the difference between two impedance values) and with the proposed perturbation method (integrating directly in a sub-domain of Ω') for both $\boldsymbol{h}-$ and $\boldsymbol{b}-$ conform formulations.

In order to avoid numerical errors due to the discretisation, the conventional technique requires exactly the same mesh for solving the problems without and with defect. However the proposed perturbation technique can be applied with two independent meshes: a mesh of the whole domain with the probe and without the flaw; a mesh of of the reduced domain with the flaw and without the explicit presence of the excitation coil. For the sake of a fair comparison, the relative error is calculated using exactly the same mesh for the two considered methods.

The relative error in the real and imaginary parts of ΔZ with respect to the solution conventionally obtained is depicted in Figs. **??** and **??** for a depth of the defect $h = 20\%$, and in Figs. **??** and **??** for a depth of the defect $h = 60\%$, for both the $\boldsymbol{h}-$ and $\boldsymbol{b}-$conform formulations. For a small error of depth $h = 20\%$, the error in the real and imaginary parts of ΔZ is smaller than 1% for $D \geq \delta$. When the depth of the defect is $h = 60\%$, one observes that in all cases the error in the real and imaginary parts of ΔZ is smaller than 1% for $D \geq 2.7\delta$ and $D \geq 2\delta$, respectively. As expected, for a given error the size of the reduced domain must be increased when the size of the defect increases.

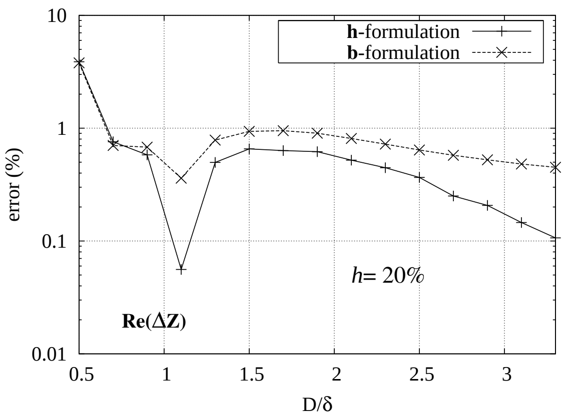

Figure 2. Relative error (%) in real part of ΔZ versus normalised size of Ω'. Defect with depth $h = 20\%$

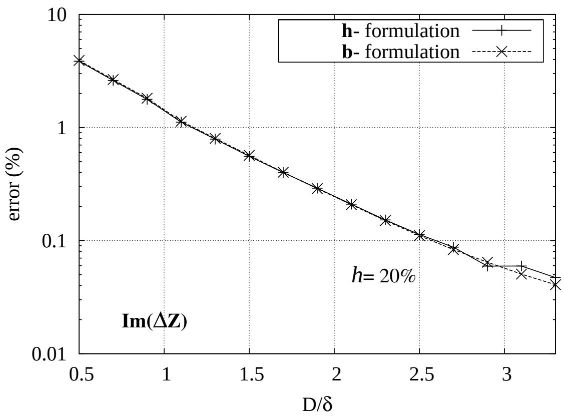

Figure 3. Relative error (%) in imaginary part of ΔZ versus normalised size of Ω'. Defect with depth $h = 20\%$

In order to validate the numerical model, we have also solved the problem in 3D with the $\boldsymbol{h}-$conform formulation and compared the results with those presented in (**?**). The locus and magnitude of the impedance change for an axial scan and different depths of the flaw are represented in Figure **??** for a rotation angle $\alpha = 0°$ and in Figure **??** for a rotation angle $\alpha = 20°$. An excellent agreement between our results and those presented in (**?**) is observed.

Conclusions

Two FE perturbation techniques based on the $\boldsymbol{h}-$ and $\boldsymbol{b}-$conform magnetodynamic formulations have been elaborated and compared. In both cases, the unperturbed field is calculated conventionally in the complete domain taking advantage of any symmetry or analytical solution (if available) and applied as a source in the flaw. Next the perturbed field is determined in a reduced domain surrounding the defect. The discretisation of this reduced domain is thus well adapted to the size of the defect and chosen independently of the dimensions of the excitation probe and the specimen under study.

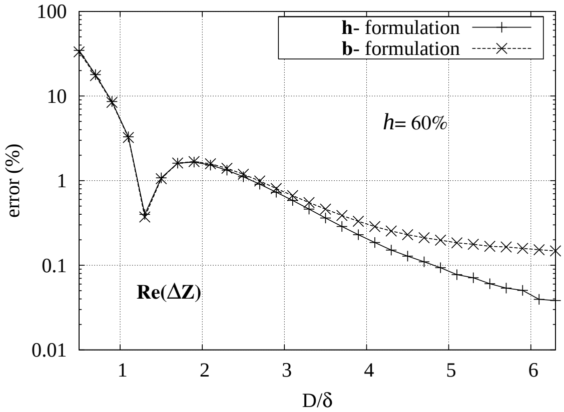

Figure 4. Relative error (%) in real part of ΔZ versus normalised size of Ω'. Defect with depth $h = 60\%$

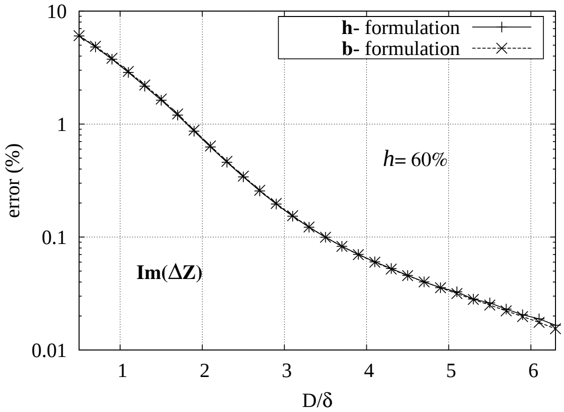

Figure 5. Relative error (%) in imaginary part of ΔZ versus normalised size of Ω'. Defect with depth $h = 60\%$

Furthermore, the impedance variation due to the presence of the flaw is calculated by performing an integral over the defect and a layer of elements in the exterior domain that touch its boundary. Therefore no integration of any flux variation in the coils is required.

The accuracy of the model has been evidenced by comparing the results obtained for different dimensions of the reduced domain to those achieved in the conventional way. The required size of the reduced domain increases with the size of the defect in hand. Finally, the solution of the 3D eddy current benchmark problem validates the presented perturbation scheme.

References

Bowler, J. R. and Jenkings, S. A. (1991), ‘Eddy-current probe impedance due to a volumetric flaw’, *Journal of Applied Physics* **70**(3), 1107–1114.

Dular, P., Kuo-Peng, P., Geuzaine, C., Sadowski, N. and Bastos, J. P. A. (2000), ‘Dual magnetodynamic formulations and their source fields associated with massive and stranded inductors’, *IEEE Transactions on Magnetics* **36**(4), 1293–1299.

Ida, N. and Lord, W. (1985), ‘A finite element model for three-dimensional eddy current NDT phenomena’, *IEEE Transactions on Magnetics* **21**(6), 2635–2643.

Michelsson, O. and Uhlmann, F. H. (2000), ‘A boundary-integral based forward solution for eddy current nondestructive testing’, *IEEE Transactions on Magnetics* **36**(4), 756–759.

Prémel, D., Pichenot, G. and Sollier, T. (2004), ‘Development of a 3D electromagnetic model for eddy current tubing inspection: application to the simulation of probe eccentricity’, *Int. J. Appl. Electromag. Mech.* **19**(1-4), 521–525.

Sabariego, R. V. and Dular, P. (2006), A perturbation technique for the finite element modelling of non-destructive eddy current testing, *in* ‘Electromagnetic Fields in Mechatronics, Electrical and Electronic Engineering’, Studies in Applied Electromagnetics and Mechanics, Vol. 27, A. Krawczyk, S. Wiak and X. M. Lopez-Fernandez (Eds.), IOS Press (Amsterdam), pp. 247–253.

Tian, Y., Li, Y., Udpa, L. and Udpa, S. S. (2002), Simulation of the world federation’s second eddy current benchmark problem, *in* ‘Review of Progress in QNDE’, Vol. 22, D. O. Thompson and D. E. Chimenti, Plenum, New York, pp. 1816–1823.

WFNDEC (n.d.), ‘World Federation of Nondestructive Evaluation Centers’. http://www.wfndec.org/.

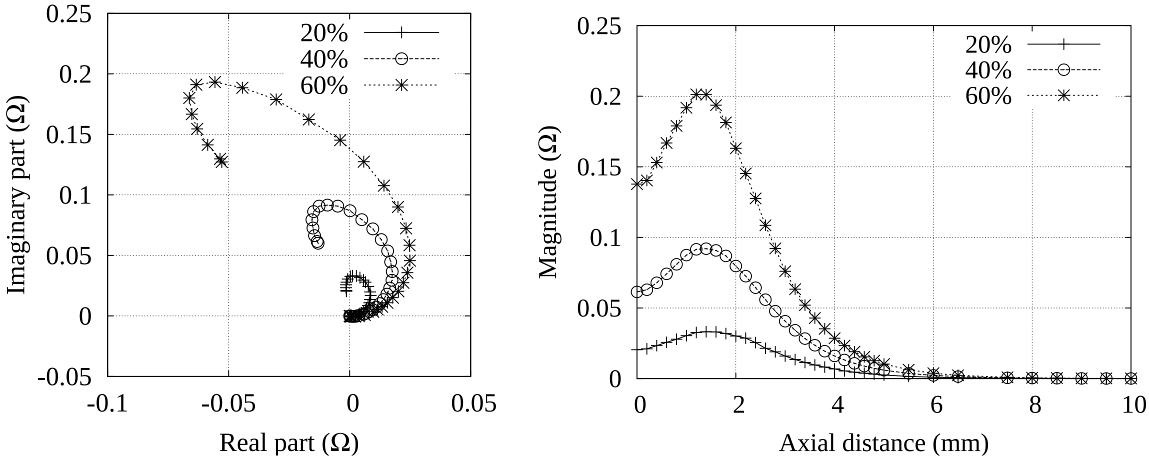

Figure 6. Locus (left) and magnitud (right) of the impedance change ΔZ for an axial scan with $\alpha = 0°$

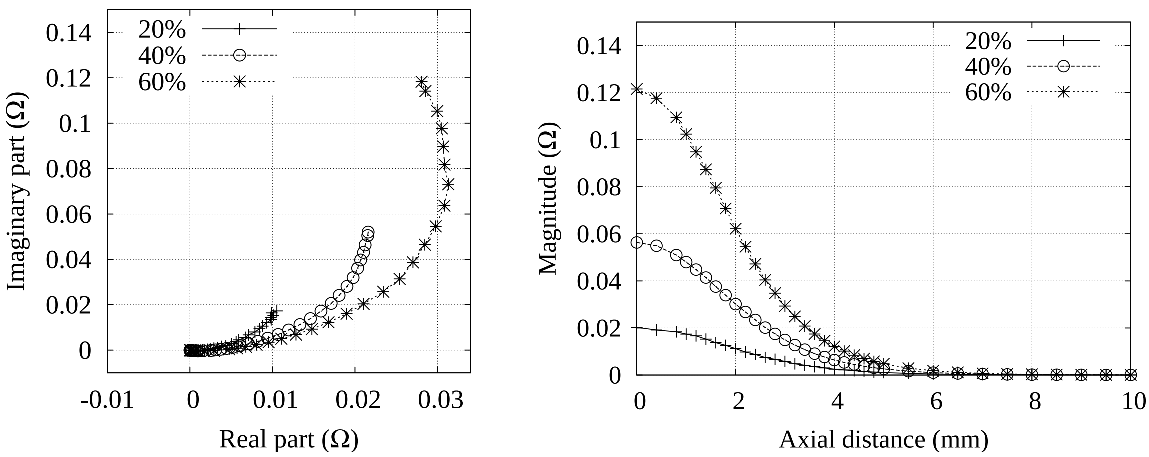

Figure 7. Locus (left) and magnitude (right) of the impedance change ΔZ for an axial scan with $\alpha = 20°$